EARTH SURFACE PROCESSES AND LANDFORMS
*Earth Surf. Process. Landforms* **34**, 1674–1684 (2009)

Published online in Wiley InterScience
(www.interscience.wiley.com) DOI: 10.1002/esp.1859

# The 'humped' soil production function: eroding Arnhem Land, Australia

**Arjun M. Heimsath,[1]* David Fink[2] and Greg R. Hancock[3]**
[1] School of Earth and Space Exploration, Arizona State University, Tempe, Arizona, USA
[2] Australian Nuclear Science and Technology Organization (ANSTO), Menai, New South Wales, Australia
[3] School of Environmental and Life Sciences, The University of Newcastle, Callaghan, New South Wales, Australia

Received 18 January 2009; Revised 24 May 2009; Accepted 1 June 2009

*Correspondence to: Arjun M. Heimsath, School of Earth and Space Exploration, Arizona State University, Tempe, AZ 85287, USA.
E-mail: Arjun.Heimsath@asu.edu

ESPL
Earth Surface Processes and Landforms

ABSTRACT: We report erosion rates and processes, determined from *in situ*-produced beryllium-10 ($^{10}$Be) and aluminum-26 ($^{26}$Al), across a soil-mantled landscape of Arnhem Land, northern Australia. Soil production rates peak under a soil thickness of about 35 cm and we observe no soil thicknesses between exposed bedrock and this thickness. These results thus quantify a well-defined 'humped' soil-production function, in contrast to functions reported for other landscapes. We compare this function to a previously reported exponential decline of soil production rates with increasing soil thickness across the passive margin exposed in the Bega Valley, south-eastern Australia, and found remarkable similarities in rates. The critical difference in this work was that the Arnhem Land landscapes were either bedrock or mantled with soils greater than about 35 cm deep, with peak soil production rates of about 20 m/Ma under 35–40 cm of soil, thus supporting previous theory and modeling results for a humped soil production function. We also show how coupling point-specific with catchment-averaged erosion rate measurements lead to a better understanding of landscape denudation. Specifically, we report a nested sampling scheme where we quantify average erosion rates from the first-order, upland catchments to the main, sixth-order channel of Tin Camp Creek. The low (~5 m/Ma) rates from the main channel sediments reflect contributions from the slowly eroding stony highlands, while the channels draining our study area reflect local soil production rates (~10 m/Ma off the rocky ridge; ~20 m/Ma from the soil mantled regions). Quantifying such rates and processes help determine spatial variations of soil thickness as well as helping to predict the sustainability of the Earth's soil resource under different erosional regimes. Copyright © 2009 John Wiley & Sons, Ltd.

KEYWORDS: $^{10}$Be; sediment transport; erosion; soil; weathering

## Introduction

Quantifying the rates of Earth surface processes across soil-mantled landscapes is critical for many disciplines (Anderson, 1994; Bierman, 2004; Dietrich *et al.*, 2003; Dietrich and Perron, 2006). Balances between soil production and transport determine whether soil exists on any given landscape, as well as how thick it might be. Soil presence and thickness, in turn, helps support much of the life that we humans are familiar with, play important roles in the hydrologic cycle, and are coupled with processes that impact the atmosphere. As such, the near-surface environment that includes soil and its parent material has become known as the Critical Zone (CZ) (Amundson *et al.*, 2007; Anderson *et al.*, 2004; Anderson *et al.*, 2007; Brantley *et al.*, 2007). Over the last 10 years significant progress, in the field (e.g. Anderson and Dietrich, 2001; Burkins *et al.*, 1999; White *et al.*, 1996; Yoo *et al.*, 2007), laboratory (e.g. White and Brantley, 2003), and with modeling (e.g. Minasny and McBratney, 2001; Mudd and Furbish, 2006) enables a new level in understanding how forces of sediment production and transport shape landscapes and help determine the viability of the Earth's soil resource (Montgomery, 2007). Despite this progress, there are significant gaps in our understanding of this interface between humans, the atmosphere, biosphere, and lithosphere. One of the most significant gaps is quantifying what controls soil thickness (Anderson *et al.*, 2007; Brantley *et al.*, 2007), while another is the continued quantification of the sediment transport relationships (cf. Geomorphic Transport Laws, Dietrich *et al.*, 2003; Heimsath *et al.*, 2005). We focus this study on a soil-mantled, upland landscape in northern Australia to quantify soil production and transport rates for a landscape shaped by a very different climatic and tectonic regime than any landscape used previously for similar landscape process studies.

Here we quantify a 'humped' soil production function with field-based measurements of cosmogenic beryllium-10 ($^{10}$Be) and aluminum-26 ($^{26}$Al) in saprolite and rock samples, where the peak soil production rate occurs under a thin soil mantle. Since Gilbert's first suggestion that soil production should depend on overlying soil thickness (Gilbert, 1877) there has been much discussion of both the theory (e.g. Carson and Kirkby, 1972; Cox, 1980) and the field evidence (e.g. Heimsath *et al.*, 1997; Small *et al.*, 1999; Wilkinson *et al.*, 2005) for how sediment production is governed by the overlying soil thickness. Although Small *et al.* (1999) and Wilkinson *et al.* (2005) report data suggestive of a peak rate beneath finite soil depth,

both report roughly uniform sediment production rates with only the suggestion of a 'humped' function as discussed extensively in Wilkinson and Humphreys (2005). Small *et al.* (1999) focus on an alpine summit flat, above a deep trough carved during past glaciations, where the gently sloping landscape is punctuated by tors and mantled with nearly constant veneer of scree-like sediment. While Small *et al.* (1999) report uniform rates of regolith production, their data are used to support a 'humped' function through a modeling effort by Anderson (2002). Wilkinson *et al.* (2005) focus on the dramatic landscape of the Australian Blue Mountains, where rocky spurs exhibit bands of exposed bedrock and pagodas. For this landscape the dramatic change between soil-mantled and bedrock dominated morphology was compared to the Oregon Coast Range of Heimsath *et al.* (2001b) and the south-eastern Australia highlands of Heimsath *et al.* (2001a) to suggest using rates from both unweathered bedrock and saprolite to define a 'humped' function (Wilkinson and Humphreys, 2005). The landscape used for this study is, in contrast, a forest-grassland region where the convex-up ridges are smoothly soil mantled and free from widespread tors or rocky cliffs.

We compare rates of soil production directly to catchment-averaged erosion rates to help constrain the erosion rates of a landscape used as a proxy for an active uranium mine in northern Australia (Hancock *et al.*, 2003; Hancock *et al.*, 2000). We also compare the 'humped' function quantified here with the exponential decline in soil production rates with increasing soil thicknesses previously reported from south-eastern Australia (Heimsath *et al.*, 2000; Heimsath *et al.*, 2006) to discuss the potential implications of changing climate or land use on the soil resource.

## Conceptual Framework and Methods

The problem of quantifying landscape evolution is tackled here by applying the well-developed mass-balance approach initially articulated by Gilbert (1877), quantitatively laid out by Culling (1960, 1965), and eloquently made accessible to a broad audience by Carson and Kirkby (1972). This conceptual framework was extensively applied to quantify soil production (e.g. Heimsath *et al.*, 1997, 1999), landscape evolution (e.g. Dietrich *et al.*, 1995), as well as model the dynamic responses of the land surface to changes in climate and tectonic forcing (e.g. Tucker and Slingerland, 1997; van der Beek and Braun, 1999). Specifically, we are interested in the vertical lowering rate of the land surface. For a bedrock surface, this rate is simply the erosion rate of the surface. For a soil-mantled landscape in local steady state, this is the rate of conversion of the underlying weathered bedrock to mobile material: the soil production rate. Soil production rates have long been hypothesized and only recently documented to decline exponentially with increasing soil thickness in a relationship termed the soil production function (Heimsath *et al.*, 1997). Field verification of this function helps quantify recent landscape evolution models (Dietrich *et al.*, 2003), and the local steady-state soil thickness assumption (soil production rates only equal total erosion rates if local soil thickness is roughly constant over time) was verified at one of the field areas initially explored in south-eastern Australia (Heimsath *et al.*, 2000).

The focus here is on hilly soil-mantled landscapes where the bedrock is actively converted to a continuous soil mantle (also referred to as regolith – the difference being that we define soil as the physically mobile layer). Importantly, the underlying saprolite, or weathered bedrock, is conceptualized as bedrock with the criterion that geomorphic processes do not physically mobilize it: it retains relict rock structure. When conditions of local steady state are assumed, the soil production rate equals the erosion rate and the local soil thickness remains temporally constant (Heimsath *et al.*, 1999). The bedrock–soil interface lowers spatially at the soil production rate, and the soil acts as a continuously dynamic layer of locally constant thickness as sediment produced is removed whilst that produced upslope is transported downslope such that the lowering rate of the bedrock–soil interface is equivalent to the landscape-lowering rate. Importantly, this rate can vary across the landscape, as discussed later, such that the landscape is not lowering at the same rate everywhere and is, therefore, out of the dynamic equilibrium discussed by Ahnert (1967, 1987).

Conversely, for bedrock-dominated landscapes, where the morphology may not be smoothly convex-up (one of the criteria enabling the steady-state erosion assumption), careful field and sample site selection becomes critical. At one extreme is a cliff-dominated landscape where the dominant process of erosion is massive block failure (e.g. Matmon *et al.*, 2005). At another extreme is the smooth, low relief, inselburg-dominated landscape where the erosional processes are clearly grain-to-grain spallation (e.g. Bierman and Caffee, 2002). Rates of erosion can mean different things across such extremes, depending on the time-scale of interest and prevailing chemical and physical processes. For example, for cliff-dominated landscapes, all bedrock surfaces (cliff face, as well as flat-lying bedrock surface above the cliff) are likely to be eroding by grain-grain spallation, although the cliff-face will also periodically fail catastrophically. The long-term retreat rate of the cliff is thus likely to be significantly greater than the lowering rate of the overall land surface. Total mass loss from the watershed draining such a landscape will include some combination of such disparate rates, including solution loss through chemical weathering as well as the fluvial transport of material physically removed from the cliff faces.

Differences between soil-mantled and bedrock-dominated landscapes become especially important when applying the methodology that we use here: *in situ*-produced cosmogenic nuclides ($^{10}$Be and $^{26}$Al). These nuclides are used extensively to quantify point-specific bedrock erosion (e.g. Lal, 1991; Nishiizumi *et al.*, 1991), soil production (e.g. Heimsath *et al.*, 1997; Small *et al.*, 1999; Wilkinson *et al.*, 2005), and spatially averaged regional rates of erosion (e.g. Bierman and Steig, 1996; Brown *et al.*, 1995; Granger *et al.*, 1996). Concentrations of these nuclides accumulate in materials at or near the Earth's surface as cosmic rays bombard atoms, such as silicon (Si) and oxygen (O) target atoms in quartz and other minerals in rock and sediments (Lal and Arnold, 1985; Lal and Peters, 1967) resulting in *in situ* formation of $^{26}$Al and $^{10}$Be, respectively. Cosmic ray production of nuclides is offset by radioactive decay of the nuclides in surfaces that are not eroding and by removal of the target material in eroding surfaces. At secular equilibrium production balances loss via erosion and decay, such that saturation concentrations of cosmogenic nuclides are effectively determined by the magnitude of the erosion rate. Application of cosmogenic nuclides to understanding landscapes is well and extensively reviewed (e.g. Bierman, 1994; Cockburn and Summerfield, 2004; Gosse and Phillips, 2001; Lal, 1988; Nishiizumi *et al.*, 1993).

Nuclide concentrations measured in quartz reflect the exposure history of a sample collected from the Earth's surface, and are dependent on the production and decay rates of the nuclide, as well as the erosion rate of the sample (Lal, 1988; Lal and Arnold, 1985; Nishiizumi *et al.*, 1991; Nishiizumi *et al.*, 1986). Similarly, nuclide concentrations accumulated in river or catchment sediments are used to infer catchment-



DOI: 10.1002/esp

averaged steady-state erosion rates assuming relatively short transport times and relatively homogeneous catchment lithology (e.g. Granger *et al.*, 1996; Bierman and Steig, 1996). We determine erosion rates in three different ways. (1) For exposed bedrock showing field evidence of eroding by grain-grain spallation or by exfoliating in thin sheets we sample the outermost centimeter or two. The nuclide concentration in these samples quantify the steady-state erosion rate of the exposed bedrock surfaces assuming that samples have had simple exposure histories and have been eroding at nearly constant rates. (2) For soil production rates, we follow the typical geomorphic transect from bedrock exposed at convex ridge crests onto the soil-mantled part of the landscape and dig soil pits to sample the top centimeter or two of saprolite or weathered bedrock directly beneath different depths of the relatively thin (< 1 m) soil cover. Nuclide concentrations from these samples are used with a corrected nuclide production rate that accounts for the shielding by the soil mantle above the sampled layer, and the local slope of the sample site, to yield a soil production rate, which is equivalent to a landscape-lowering rate (for details see Heimsath *et al.*, 1999). (3) We also collect stream and creek sediments and use the nuclide concentrations to infer a catchment-averaged erosion rate. Each of these applications depends on careful geomorphic site selection such that the assumptions and simplifications detailed in the earlier referenced studies are met.

## Field Site

Work for this study was done to expand on previous work across an extensively examined field site adjacent to Tin Camp Creek. We collected bedrock, saprolite, and catchment sediment samples to determine the spatial variability of erosion rates across a landscape used to model landscape evolution in the context of the uranium mining industry interests in the region (Hancock and Evans, 2006; Hancock *et al.*, 2008a; Hancock *et al.*, 2008b) (Figure 1). The presence of Energy Resources Australia Ranger Mine (ERARM) for uranium in a catchment with similar geology, hydrology and erosional history as the Tin Camp Creek region has driven much research in Tin Camp Creek in order to establish a natural baseline of erosion rates and geomorphic processes for the area. The region typically receives seasonal rainfall of about 1400 mm/y between October and April, with short, high-intensity storms that are normal for the tropical environments of northern Australia.

The field site is part of the Ararat Land System (Story *et al.*, 1976), where the landscape is developing by the retreat of the Arnhem Land escarpment over the last few million years. Our study region is essentially a basin carved into the rocky highlands of this ancient sandstone with a main ridge, about as high as the surrounding highlands, bisecting the basin. Our sampling scheme was to traverse this ridge, sampling both exposed and unweathered bedrock as well as collecting weathered rock from below a range of soil depths to test the soil-production conceptual framework across such a radically different geographic region compared to previous work on soil production and landscape evolution. Soils are mostly red loamy earths and shallow gravelly loams with some micaceous silty yellow earths and minor solodic soils on the alluvial flats (Riley and Williams, 1991). We focused on the upland, soil-mantled hillslopes, where soils were either greater than about 30 to 40 cm thick or absent (Figure 2). Bedrock outcropping across the hills was competent and significantly less weathered than the saprolite beneath the soil mantle (Wells *et al.*, 2008), although we did not collect samples for chemical weathering studies. Vegetation is an open dry-sclerophyll forest with abundant seasonal grassland interspersed throughout.

Burrowing native animals did not seem as abundant as they are in the Bega Valley escarpment region (Heimsath *et al.*, 2000; Heimsath *et al.*, 2006), but previous studies examining gullies (Hancock *et al.*, 2000; Riley and Williams, 1991; Saynor *et al.*, 2004; Townsend and Douglas, 2000) highlight the potential role of feral water buffalo and pigs in disrupting the soil mantle, as well as frequent fire due to Aboriginal burning over the last 40 000 years or so (Figure 3) leading to increased tree throw processes of soil production and transport. The area is also subject to intense cyclonic activity and in April 2006 a Category five cyclone occurred in the catchment resulting in considerable tree-throw. The majority of these fallen trees die and are burnt or are eaten by termites in subsequent seasons. An extensive study in the region and also in the study catchment found that trees when pushed over exposed pits on average 30 cm deep ($\sigma$ = 18 cm) and 67 cm wide ($\sigma$ = 56 cm) (Staben and Evans, 2008; Saynor *et al.*, 2009). Despite the shallow slumping shown in Figure 3, and the low gully initiation thresholds found by Hancock and Evans (2006), we were able to focus our soil production rate sampling strategy entirely on smoothly convex-up soil-mantled hillslopes similar to that shown in Figure 2 that fit the conceptual framework summarized earlier. The surface stone lag visible in the two photographs suggests that post-fire overland flow might winnow away fine surficial sediments, but the absence of flow deposits and the convex-up morphology of the hillslopes leads us to infer that overland flow is not the dominant sediment transport processes for this landscape. Instead, when combined with our observations of quartz clasts throughout the soil profiles examined for this study, we infer that bioturbation results in a homogenization of the soil profiles and a downward transport of soils as well as quartz clasts, similar to that discussed by Wilkinson and Humphreys (2005), reviewed in Gabet *et al.* (2003), and quantified by Kaste *et al.* (2007) for other landscapes.

## Results and Discussion

We collected 23 samples for cosmogenic $^{10}$Be and $^{26}$Al analyses from across the study area (Figure 1C, Table I). Bedrock, soil and sediment samples were prepared following the methods reported by Child *et al.* (2000) and measured at the Accelerator Mass Spectrometry (AMS) ANTARES facility at ANSTO (Fink and Smith, 2007). $^{10}$Be results given in Table I for this work have been normalized using the NIST SRM 4325 standards with a nominal value of 30 200×10$^{-15}$ and for $^{26}$Al using PRIME $^{26}$Al standards Z93–0221 with a nominal value of 16 800×10$^{-15}$. We report concentrations for both $^{10}$Be and $^{26}$Al because sample lithology and exposure history were not previously constrained. The availability of $^{26}$Al data can provide confirmation of assumptions of continuous exposure for bedrock samples, and in some cases identification of samples undergoing complex exposure or burial (e.g. long-term storage of stream sediments or surface stripping followed by soil mantling) (Nishiizumi *et al.*, 1993). Site-specific production rates computed from scaling factors and calibration production rate values for sea-level and high latitude (SLHL) were recently revised and summarized (Balco *et al.*, 2008). In addition, new values were reported for both the $^{10}$Be half life and $^{10}$Be/$^{9}$Be ratios of calibration standards used in AMS for $^{10}$Be measurements. (Nishiizumi *et al.*, 2007; Fink and Smith, 2007). For the data in Table I, we used the scaling scheme of



DOI: 10.1002/esp

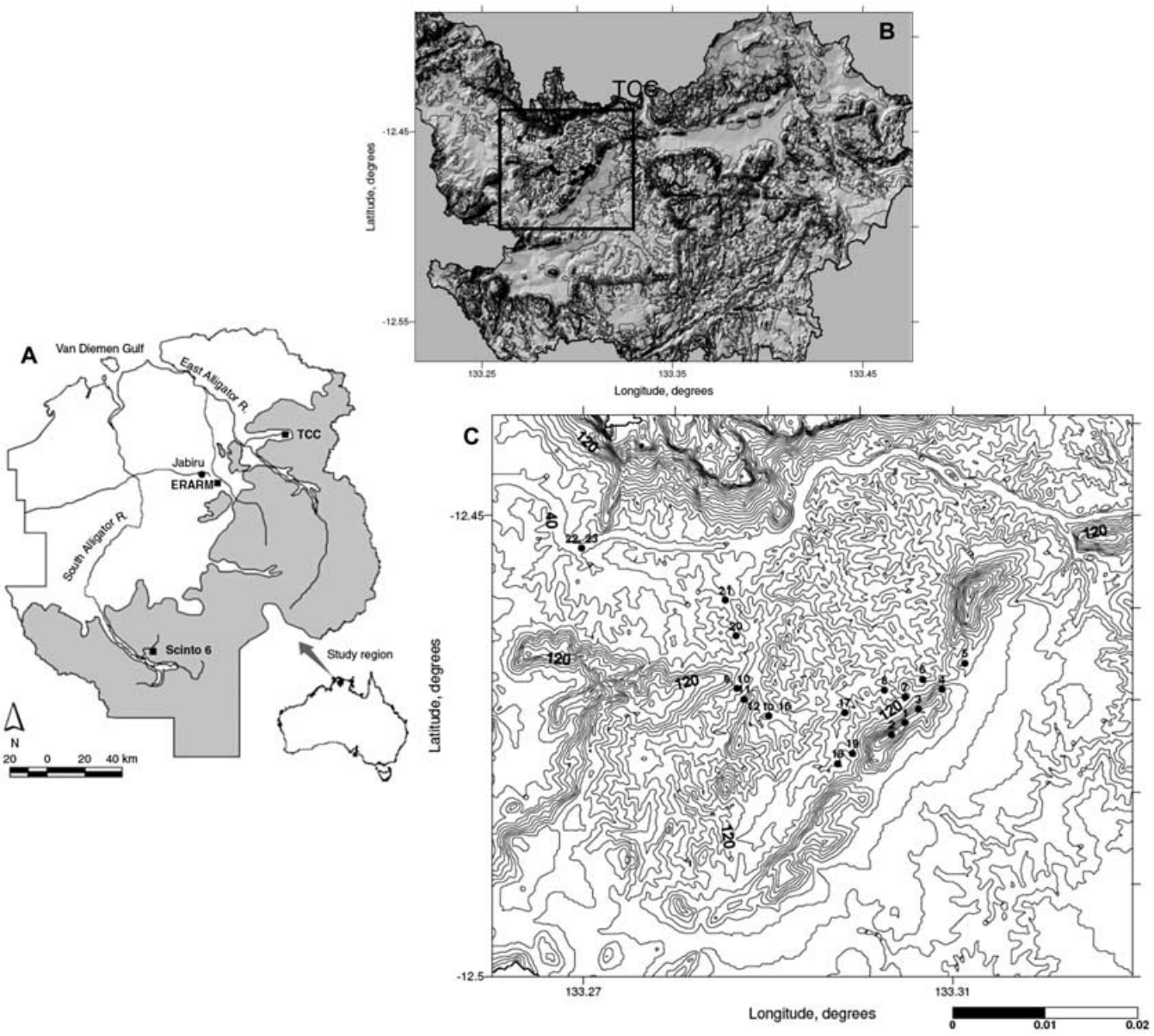


**Figure 1.** (A) Field map of the region in Australia's Northern Territory showing the location of the Tin Camp Creek (TCC) site in relation to the Energy Resources Australia Ranger Mine (ERARM) for uranium. The Arnhem Land Plateau is shaded in grey, showing the regional erosion into the stony plateau typified by our field area. (B) Shaded relief map of the region immediately surrounding the study area, showing the prominence of the main ridge where the bedrock samples were collected and the relation of the soil-mantled, upland landscapes of this study to the rocky highlands of the surrounding Arnhem Land Plateau, indicated with grey. Black outline delineates area shown by topography in (C). (C) Topographic map of the area surrounding our field site. Contour intervals are 10 m and are generated from the one-second digital elevation model (DEM) of the region provided by the Defense Imagery and Geospatial Organization. Sample locations shown by black dots labeled with TC sample number.

Stone (2000) with a SLHL production rate of 5·1 and 31·1 atoms/g/y for $^{10}$Be and $^{26}$Al respectively. A comparison of results for paired $^{10}$Be and $^{26}$Al erosion rates are in agreement and internally consistent within one-sigma errors [apart from Tin Camp sample number 12 (TC-12)]. For samples where excessive boron contamination was measurement we applied correction factors to account for this and as a conservative measure we have applied an additional 10% error to their $^{10}$Be data. $^{10}$Be data for sample TC-19 was rejected due to unacceptable boron contamination, which was not available for correction using our normal procedures. Three samples for $^{26}$Al (TC-3, 5, and 21) failed to provide a usable ion-source beam for AMS measurement. Calculation of final soil production, bedrock erosion rates and basin-averaged rates are based, where available, on linear averages of the two nuclide results for each sample.

First, nuclide concentrations from samples noted as BRK (for bedrock) in Table I are used to infer steady-state erosion rates, ranging from 5 to 11 m/Ma, from exposed bedrock surfaces. Second, concentrations measured in the weathered bedrock directly beneath an actively eroding upland soil mantle, with depths noted in Table I, are used to infer steady-state soil production rates. Soil production rates inferred from these samples range from 23 to 11 m/Ma with depths from 35 to 70 cm. Finally, concentrations from stream sediments, noted as Sed in Table I, are used to determine average erosion rates from drainage basins of different sizes, from the ephemeral first-order drainages off the main ridge in the study area to the entire catchment drained by Tin Camp Creek, and range from 4 to 31 m/Ma. Rates inferred from these sediment samples from various locations reflect the average of all processes active in the basin contributing to the sample point.



DOI: 10.1002/esp

**Figure 2.** Photograph showing the typical convex-up hillslope of the soil mantled upland landscape of the study area. Landscape is barren as photograph is taken soon after a local fire. View shows the rocky cliffs on the horizon that mark the edge of the Arnhem Land Plateau. This figure is available in colour online at www.interscience.wiley.com/Journal/espl

**Figure 3.** Photograph showing shallow slump feature in a concave-up, unchanneled swale soon after the same fire that denuded the landscape shown in Figure 2. Discussed in Hancock and Evans (2006). Stony lag of colluvial quartz clasts visible on the soil surface (see text). This figure is available in colour online at www.interscience.wiley.com/Journal/espl

## Soil production and bedrock erosion

Seven samples of weathered bedrock beneath different local soil depths follow an exponential decline of soil production rates with increasing soil thickness (Figure 4). Using these samples alone (TC-9–TC-15) to quantify a soil production function results in a variance-weighted function that is remarkably similar to the function quantified in south-eastern Australia (Heimsath *et al.*, 2000; Heimsath *et al.*, 2006):

$$\mathrm{SPR} = (47 \pm 15)\mathrm{e}^{-(0{\cdot}020 \pm 0{\cdot}007)H} \quad (1)$$

where SPR is the soil production rate (in m/Ma), $H$ is the overlying soil thickness (in centimeters), and the fitted constants have units of m/Ma and $\mathrm{cm}^{-1}$, respectively.

Specifically, when the rates of exposed bedrock erosion are considered, averaging about 8 ± 2 m/Ma (Figure 4, Table I, samples TC-1–TC-5 and excluding TC-16 which is discussed later), then the shape of the soil production function is more reasonably defined as being 'humped' (after Carson and Kirkby, 1972; Cox, 1980). These data thus confirm a hypothesized soil production function with only limited empirical support [see discussions in Wilkinson and Humphreys (2005) and Humphreys and Wilkinson (2007)]. Following the initial intuition of Gilbert (1877), there are only two field-based studies apart from Heimsath and colleagues (Heimsath *et al.*, 2001a; Heimsath *et al.*, 2001b) that we know of that show support for soil production rates reaching a maximum under a finite soil cover. Small *et al.* (1999) use $^{10}$Be to show that sediment production beneath 90 cm of scree-like sediment is about twice as great as the erosion rates of bare bedrock surfaces for their alpine landscape in the Wind River Range of Wyoming, USA. Wilkinson *et al.* (2005) also use $^{10}$Be concentrations from samples across a heath and forested landscape of the Blue Mountains of Australia to suggest higher rates under thin heath soil than for exposed bedrock although the corrected data (see Erratum associated with the study) show that rates are roughly similar across the landscape. The suggestion of a 'humped' function was only possible by introducing a hypothetical soil cover that was stripped before 10 ka (Wilkinson *et al.*, 2005). Thus, although a robust quantification of a 'humped' function was elusive, discussion of their results (Wilkinson and Humphreys, 2005), as well as the modeled results of Anderson (2002), have furthered the hypothesis that maximum soil production rates occur beneath some finite soil depth rather than from exposed bedrock. Our data offer support for this model, and are strengthened by the morphology of the site.

A critical instability exists for a humped soil production function, as discussed lucidly by Carson and Kirkby (1972) and shown in the modeling results of Dietrich *et al.* (1995). Although Wilkinson and Humphreys (2005) question the validity of this modeling effort, using the argument of a non-uniform diffusivity parameter noted by Anderson (2002), the morphologic signature of this instability appears to be supported at some study areas. Namely, that if there is a decline of soil production rates from the peak under some finite soil cover to a lower rate for exposed bedrock, then the landscape is either going to have outcropping bedrock or soil depths greater than the finite depth defining the maximum soil production rate. Heimsath *et al.* (2001a) showed a suggestion of this pattern across the highlands of south-eastern Australia and built on the modeling effort of Dietrich *et al.* (1995) to model the emergence of tors across the landscape and conclude that the widespread outcropping bedrock surfaces were incipient tors. From a very different field location in the Oregon Coast Range, Heimsath *et al.* (2001b), also reported lower rates of erosion from exposed bedrock samples. That study concluded, however, that an exponentially declining soil production function was most appropriate for the landscape because of how chemical weathering segregated the landscape into unweathered outcropping sandstone ridge crests and a highly weathered saprolite being physically mobilized to a colluvial soil (Anderson and Dietrich, 2001). Furthermore, the study suggested a long-term steady-state in landscape erosion for the region because of the similarity in erosion rates between the catchment-averaged rates, the low rates from exposed bedrock, and the range of soil production rates from weathered saprolite samples. In such a steady-state scenario soil production rates from different weathered states of bedrock are roughly equal, providing empirical support for the hypothesized equilibrium scenario modeled, for example, by Ahnert (1987).

The shallowest soil thickness that we measured across the Tin Camp Creek field site was about 35 cm, not including the very thin soils near outcropping bedrock patches. Although we do not have extensive soil depth measurements mapped across the landscape (e.g. Heimsath *et al.*, 2001a; Heimsath *et al.*, 2001b), our observations do support the suggestion given earlier that a landscape governed by a humped soil



DOI: 10.1002/esp

**Table I.** Erosion rates from cosmogenic nuclide concentrations

| Sample | Type/depth[b] | Weight (g) | Carrier (mg) | $^{10}$Be ($10^6$ atom/g) | ± | $^{26}$Al ($10^6$ atoms/g) | ± | $^{26}$Al/$^{10}$Be | Production rate[c] | Elevation (m) | $E^d$ ($^{10}$Be) (m/Ma) | ± | $E^c$ ($^{26}$Al) (m/Ma) | ± | $E$ average (m/Ma) | ± | Minimum exposure age (ka) |
|---|---|---|---|---|---|---|---|---|---|---|---|---|---|---|---|---|---|
| TC-1 | BRK | 40·856 | 0·489 | 0·300 | 0·014 | 2·351 | 0·287 | 7·8 | 0·689 | 220 | 6·3 | 0·4 | 4·5 | 0·6 | 5·4 | 0·8 | 87 |
| TC-2 | BRK | 45·216 | 0·507 | 0·228 | 0·014 | 1·354 | 0·177 | 5·9 | 0·689 | 220 | 8·3 | 0·7 | 8·2 | 1·2 | 8·3 | 1·4 | 66 |
| TC-3 | BRK | 49·998 | 0·499 | 0·165 | 0·012 | | | | 0·682 | 208 | 11·4 | 1·0 | | | 11·4 | 1·0 | 48 |
| TC-4 | BRK | 47·018 | 0·493 | 0·208 | 0·010 | 1·400 | 0·265 | 6·7 | 0·673 | 191 | 8·9 | 0·7 | 7·8 | 1·6 | 8·3 | 1·7 | 61 |
| TC-5 | BRK | 51·355 | 0·496 | 0·265 | 0·018 | | | | 0·659 | 166 | 6·8 | 0·6 | | | 6·8 | 0·6 | 80 |
| TC-6 | Sed-1st | 47·083 | 0·505 | 0·154 | 0·010 | 0·732 | 0·104 | 4·8 | 0·648 | 144 | 11·7 | 1·0 | 14·7 | 2·2 | 13·2 | 2·4 | 47 |
| TC-7 | Sed-1st | 48·861 | 0·510 | 0·159 | 0·007 | 0·643 | 0·289 | 4·0 | 0·632 | 114 | 11·0 | 0·8 | 16·4 | 7·7 | 13·7 | 7·7 | 50 |
| TC-8 | Sed-2nd | 44·376 | 0·409 | 0·117 | 0·007 | 0·652 | 0·166 | 5·6 | 0·621 | 93 | 14·7 | 1·2 | 15·9 | 4·2 | 15·3 | 4·4 | 37 |
| TC-9 | 40 cm | 47·904 | 0·419 | 0·056 | 0·004 | 0·369 | 0·043 | 6·6 | 0·404 | 93 | 20·4 | 1·9 | 18·3 | 2·3 | 19·3 | 3·0 | 27 |
| TC-10 | 45 cm | 49·029 | 0·399 | 0·054 | 0·008 | 0·273 | 0·030 | 5·1 | 0·390 | 88 | 20·3 | 3·3 | 24·1 | 2·8 | 22·2 | 3·0 | 27 |
| TC-11 | 70 cm | 48·975 | 0·405 | 0·086 | 0·013 | 0·435 | 0·062 | 5·1 | 0·318 | 97 | 10·2 | 1·6 | 12·1 | 1·8 | 11·1 | 2·4 | 54 |
| TC-12 | 55 cm | 48·684 | 0·404 | 0·093 | 0·012 | 0·309 | 0·077 | 3·3 | 0·369 | 123 | 11·0 | 1·5 | 20·1 | 5·1 | 15·5 | 5·3 | 50 |
| TC-13 | 50 cm | 49·568 | 0·400 | 0·139 | 0·021 | 0·832 | 0·104 | 6·0 | 0·637 | 123 | 12·7 | 2·1 | 12·7 | 1·7 | 12·7 | 2·7 | 43 |
| TC-14 | 38 cm | 49·566 | 0·395 | 0·069 | 0·011 | 0·508 | 0·078 | 7·4 | 0·637 | 123 | 25·8 | 4·3 | 21·1 | 3·4 | 23·4 | 5·5 | 21 |
| TC-15 | 35 cm | 48·855 | 0·389 | 0·059 | 0·003 | 0·444 | 0·084 | 7·5 | 0·477 | 123 | 22·8 | 1·7 | 18·0 | 3·6 | 20·4 | 3·9 | 24 |
| TC-16 | BRK | 48·751 | 0·402 | 0·075 | 0·005 | 0·438 | 0·063 | 5·8 | 0·637 | 123 | 23·9 | 2·0 | 24·6 | 3·7 | 24·3 | 4·2 | 23 |
| TC-17 | Sed-3rd | 45·580 | 0·420 | 0·148 | 0·010 | 0·666 | 0·108 | 4·5 | 0·628 | 106 | 11·8 | 1·6 | 15·7 | 2·7 | 13·8 | 3·1 | 47 |
| TC-18 | Sed-2nd | 43·668 | 0·416 | 0·179 | 0·010 | 1·074 | 0·164 | 6·0 | 0·628 | 115 | 9·7 | 1·3 | 9·5 | 1·6 | 9·6 | 2·1 | 57 |
| TC-19 | Sed-1st | 45·012 | 0·399 | | | 0·398 | 0·077 | | 0·628 | 106 | | | 26·7 | 5·3 | 26·7 | 5·3 | 72 |
| TC-20 | Sed-4th | 45·017 | 0·407 | 0·070 | 0·006 | 0·289 | 0·066 | 4·1 | 0·621 | 92 | 25·0 | 2·5 | 36·6 | 8·6 | 30·8 | 9·0 | 22 |
| TC-21 | Sed-5th | 43·432 | 0·410 | 0·088 | 0·006 | | | | 0·610 | 71 | 19·4 | 1·6 | | | 19·4 | 1·6 | 28 |
| TC-22 S | Sed-TCC | 49·178 | 0·394 | 0·260 | 0·040 | 1·607 | 0·296 | 6·2 | 0·600 | 50 | 6·3 | 1·0 | 5·9 | 1·2 | 6·1 | 1·6 | 87 |
| TC-23 P | Sed-TCC | 49·720 | 0·410 | 0·369 | 0·047 | 2·433 | 0·391 | 6·6 | 0·600 | 50 | 4·4 | 0·6 | 3·7 | 0·7 | 4·0 | 0·9 | 124 |

[a] TC, Tin Camp sample number; S, P, sand, pebbles, respectively, referring to catchment-averaged detrital sediment samples from main drainage of Tin Camp Creek (TCC).
[b] Depth is thickness of overlying soil mantle; Sed is sedimentary sample with basin order noted; BRK is bedrock exposed flush with ground surface·
[c] Production rate scaling factor to correct nuclide production for slope, soil cover (p = 1·3), elevation and latitude·
[d] All errors propagated to erosion rates, $E$; not propagated to the [$^{10}$Be]-based minimum exposure age.
Note: $^{10}$Be and $^{26}$Al production rates scaled from the high latitude, sea level rates of 5·1 and 31·1 atoms/g/y·
Blanks in data are from poor analytical return from sample processing, or poor AMS current; samples TC-10, 11 and 12 had very high boron contamination.



DOI: 10.1002/esp

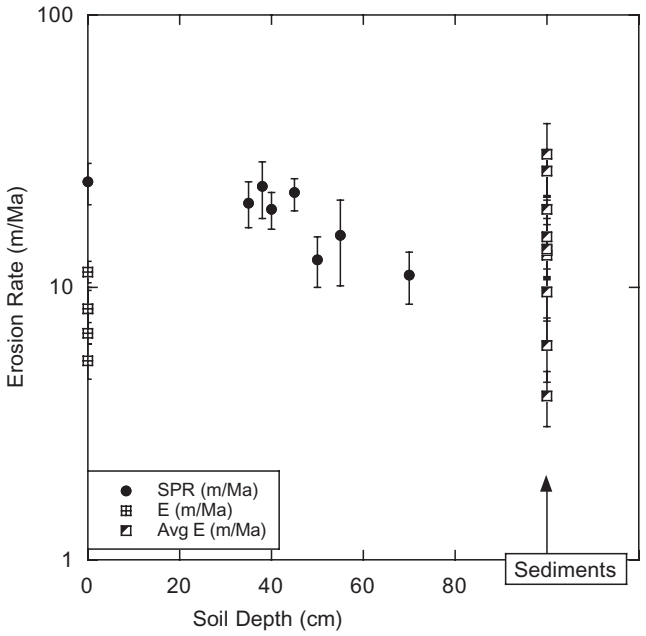


**Figure 4.** Erosion rates (average of $^{10}$Be and $^{26}$Al, m/Ma, from Table I) plotted against overlying soil thickness are considered soil production rates, and are plotted with filled black circles, along with bedrock erosion rates, plotted with crosses in open squares, and are plotted on the same graph as the catchment-averaged erosion rates, shown by the half-filled squares on the right side of the graph. Equation 1 in the text is least squares fit to the soil production rates from beneath 35 cm of soil and greater, not including the exposed bedrock samples.

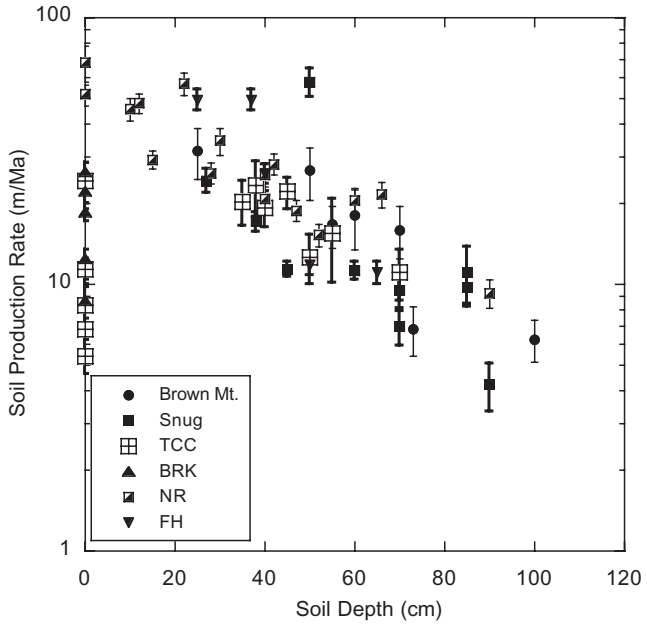


**Figure 5.** Soil production rates plotted against overlying soil thickness for data shown in Figure 4 along with the four field sites across the south-eastern escarpment (Heimsath *et al.*, 2000, 2001a; Heimsath *et al.*, 2006) (Brown Mt., highlands above escarpment; Snug, coastal lowlands; NR, Nunnock River, escarpment base; FH, Frogs Hollow, also highlands). Filled triangles are from exposed bedrock (BRK), possibly incipient tors, and are not necessarily indicative of a humped production function for the south-eastern sites. Note that the exposed samples (zero soil depth) from Tin Camp Creek (TCC) are plotted with the same symbols as the samples from beneath soil cover at TCC in this figure, and together the data suggest a lower soil production rate, which supports a humped soil production function for the TCC site.

production function is roughly divided between outcropping bedrock and soil thicknesses greater than the depth defining the maximum soil production rate. Erosion rates from the outcropping bedrock samples reveal an interesting pattern and suggest that local soil stripping events can punctuate landscape evolution of this landscape despite the relatively smooth morphology. Five samples from bedrock exposed across the bedrock dominated ridge crest of the field area (TC-1–TC-5) all define low soil production rates, averaging about 8 m/Ma (locations on Figure 1, plotted as boxed plus symbols on Figure 4, rates listed in Table I).

The single erosion rate inferred from an exposed rock sample from the region where we collected the soil production rate samples is three times as fast, 24 m/Ma (TC-16, Table I), and is roughly equal to the maximum soil production rate from beneath about 38 cm of soil (TC-14; 23 m/Ma). We differentiate this bedrock sample from the others and plot its rate with the same black filled circle as the soil production samples to suggest the potential for recent stripping of the soil cover that may have once mantled this sample. If there had been, for example, 35 cm of soil covering this sample until relatively recently, then the depth-corrected soil production rate inferred from the nuclide concentrations would be about 18 m/Ma, in line with the peak soil production rates. We emphasize that this suggestion is purely speculative, as we did not observe evidence of recent stripping events for the sampling site. Nonetheless, the nuclide concentrations measured in TC-16 emphasize that if a critical instability exists due to a 'humped' soil production function, then there are likely to be both exposed bedrock and soil mantled areas that have recently experienced or are currently experiencing locally transient rather than steady-state conditions.

When we compare the Tin Camp Creek soil production rates with those measured across the south-eastern Australia escarpment (Heimsath *et al.*, 2006) we find remarkable similarity (Figure 5). Namely, that the rates from the two dramatically different regions, climatically as well as tectonically, overlap almost entirely. Rates from south-eastern Australia are from two field sites above the escarpment [Brown Mt. and Frogs Hollow (FH)], one at the base of the escarpment [Nunnock River (NR)], and on the coastal lowlands (Snug), and include outcropping bedrock across the face of the escarpment (BRK) (Heimsath *et al.*, 2000, 2001a; Heimsath *et al.*, 2006). The only site that appears to unequivocally support a simple exponential decline of soil production with increasing soil thickness is the escarpment base at NR (Heimsath *et al.*, 2000). The absence of tors, or extensive patches of outcropping bedrock at that site, as well as the morphological support for a local steady-state soil production and transport model are striking differences between NR and the other sites across the escarpment or Tin Camp Creek.

## Average erosion rates

Nine samples of stream and creek sand quantify catchment-averaged erosion rates from across the study area (TC-6–TC-88 and TC-17–TC-23). Five samples from first- and second-order drainages off the main ridge bisecting the region (TC-6, 7, 8, 17 and 18; Figure 1C; Table I) quantify rates that average about 13 ± 2 m/Ma and are lower than the two draining the entire soil-mantled upland study area (TC-20 and TC-21) (Figure 6). TC-20 and TC-21 average ~25 m/Ma, suggesting that the highest rates of soil production are spatially widespread across the upland region and that the sediment samples reflects these rates. The near-factor-of-two difference in



DOI: 10.1002/esp

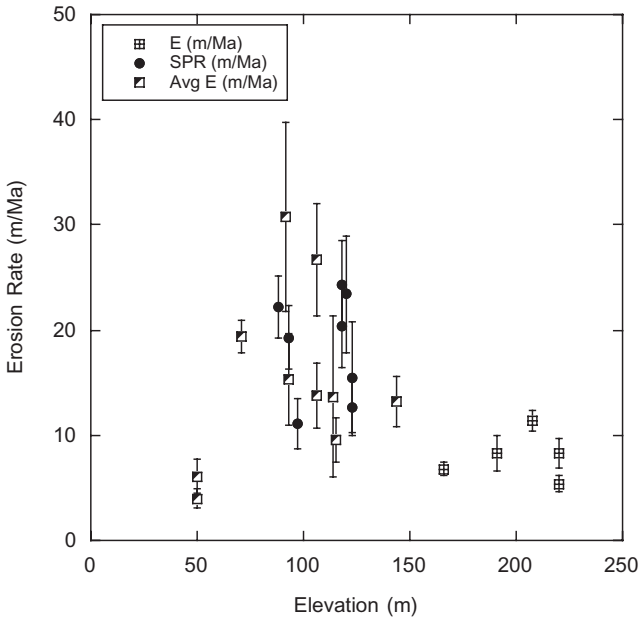


**Figure 6.** Erosion rates (equivalent to soil production rates) (in m/Ma) plotted against sample elevation for all three types of samples collected for this study – exposed bedrock erosion (*E*), soil production (SPR), and catchment averaged rates from stream sediments (Avg E). Symbols are the same as in Figure 4.

erosion rates from the prominent ridge to the low-relief uplands also suggests the creation of relief in the landscape especially when we consider the two samples from the main drainage of Tin Camp Creek (TC-22 and TC-23). These two samples yield the lowest rates from the study area, equaled only by the slowest soil production rate beneath the thickest soil cover and lowest bedrock erosion rates, averaging about 5 m/Ma. Without a detailed examination of the contributing area for these samples, which is beyond the scope of this study, we cannot fully quantify the sediment contributions resulting in such low rates. Modeling of the landscape evolution of the study region has produced landscape-lowering rates very dependent on the numerical model used and its parameterization (i.e. the SIBERIA and CAESAR models produce lowering rates of 70–170 m/Ma and 8–9 m/Ma respectively) and therefore long-term rates are speculative at present using such models (Hancock *et al.*, in press).

We can, however, posit two relatively straightforward explanations that are likely to be acting in concert. First, sediment contributions from a much larger drainage area eroding at average rates lower than 5 m/Ma are averaged with the sediment contributions from the relatively small area of our study. Given the clear agreement between the soil production and bedrock erosion rates and the corresponding sub-catchment average rates from the study area, this seems to be a plausible explanation. Specifically, we know that sediment draining the study area and contributing to the sediment in Tin Camp Creek records an average erosion rate of about 25 m/Ma as recorded by TC-20 and TC-21 (Figure 1C and Figure 6). We also know that it is likely that some of the sediment produced from the more slowly eroding main ridge, as recorded by samples TC-6, 7, 8, 17 and 18, is making it to the main channel. When all of this sediment recording rates between about 10 and 25 m/Ma is mixed with sediment being contributed from the rocky highlands drained by the main channel of Tin Camp Creek, then the average rate drops to about 5 m/Ma, as recorded by TC-22 and TC-23. Erosion rates from the rocky highlands must, therefore, be significantly lower than 5 m/Ma. The conclusion of this first explanation is, therefore, that a slowly eroding stony highland is being eroded into by the more rapidly eroding landscape characterized by the soil-production samples of our study area.

The second relatively simple explanation for the divergence in rates between the study area and the main, Tin Camp Creek basin-averaged rates is that the samples leading to the higher erosion rates (especially TC-20 and TC-21) may contain sediments exhumed from recent gullying, or more rapid erosion of the study area caused by post-fire stripping events. If this were the case, then it is possible that sediments contributing low $^{10}$Be concentrations because of exhumation from depth would lead to the inference of high erosion rates. While we know that shallow slumping occurs, as suggested by Figure 3 and the study of Hancock and Evans (2006), we also made an effort to sample for our soil production rates from regions with no evidence of shallow landsliding or other disturbances. Nonetheless, the contributing areas for TC-20 and TC-21 are large enough that our field survey and exploration did not cover the region entirely. Furthermore, an assessment using the fallout environmental radioisotope caesium-137 ($^{137}$Cs) (Hancock *et al.*, 2008a), as well as the overall denudation rates for the area (10–40 m/Ma), determined using stream sediment data from a range of catchments of different sizes in the general region (Cull *et al.*, 1992; Erskine and Saynor, 2000), suggest that these results are reasonable.

In either scenario, or both acting together, the average erosion rates from stream sediments reported here are not unreasonable and fit well with the point-specific soil production and bedrock erosion rates to quantify how erosion rates vary across the landscape. With minimum exposure ages ranging from about 20 to 120 ka (Table I), these samples are integrating the role of erosional processes operating over significant climate variations for the region. This would raise concern over the assumption of steady-state processes for other landscapes where we have applied this methodology, but this tropical upland landscape of northern Australia is unlikely to have changed drastically during the last hundred thousand years. Even if there were significant changes in dominant erosional processes during the shift from the Last Glacial Maximum to the present, the agreement between average and point-specific rates and the well-defined soil production function suggest that the cosmogenic $^{10}$Be and $^{26}$Al concentrations have attained a steady state reflecting the currently dominant processes. Comparison with short-term rates from the same catchment, quantified using fallout-derived $^{137}$Cs (Hancock *et al.*, 2008a), suggest local variations in erosion rate can exceed a factor of 10 (assuming an average saprolite bulk density of 2·0 g/cm$^3$ and converting our nuclide-based lowering rates to sediment yield rates), such that high local variability of process is captured well by the long-term signal of using cosmogenic $^{10}$Be and $^{26}$Al.

## Conclusions

Sediment production rates across the upland, soil-mantled landscape in Arnhem Land, Australia define a 'humped' soil production function, where the maximum rate of about 20 m/Ma is from beneath 35–40 cm of soil. Bedrock is exposed across the steeper uplands, but does not form significant topographic steps as it does on other soil-mantled landscapes. Sediment production rates from this exposed bedrock are significantly slower and average about 8 m/Ma. When we compare soil production rates from this tropical landscape to the temperate region of south-eastern Australia we find



DOI: 10.1002/esp

remarkable similarity in both the magnitude of the soil production rates, as well as the form of the exponential decline of the rates with increasing soil thickness. This agreement suggests that very different processes of soil production (tree throw versus burrowing wombats as the potential dominant process, respectively) can lead to similarity in the decrease of soil production with increasing soil depth. While there is no significant animal burrowing at Tin Camp Creek, tree throw and the resultant shallow pit-mounds as a result of cyclonic activity is a potentially significant driver of soil production and transport. A logical next step to further resolve both the shape of the soil production function for a tropical landscape with no tectonic forcing, as well as gain understanding into why the rates are roughly equal to rates from a temperate landscape with clear tectonic forcing, is to pursue a detailed study of the chemical weathering of soils and saprolite across the Tin Camp Creek field area. Combining this with measurements of fallout-derived isotopes in the soils will help expand our understanding of sediment production and transport processes.

Catchment-averaged rates from small catchments draining directly the soil-mantled slopes agree well with the soil production rates, while rates from the main drainage of Tin Camp Creek include the stony highlands and are much slower at about 5 m/Ma. We also show agreement between the more slowly eroding bedrock ridge crest of the main ridge bisecting the study area and the catchment averaged rates from small basins draining directly from this ridge. By coupling point-specific with catchment-averaged sampling we therefore gain a more complete understanding for the erosional processes active across this northern region of Australia.

*Acknowledgements*—We thank the traditional landowners of the study site, The Northern Land Council, and Supervising Scientist Division of the Department of Environment, Water Heritage and Arts staff, especially Brian Smith, for their help. J. Lowry provided the digital elevation used for Figure 1. Data from the Defense Imagery and Geospatial Organization, through Geoscience Australia. We thank AFMECO Mining and Exploration Pty Ltd. and Cameco Australia Pty Ltd. (J. Parks, G. Otto and staff) for their support. This project was funded by AINSE Grant 522 and 04/004 and NSF-EAR-0239655. Reviews by S. Mudd and M. Wilkinson improved this manuscript.

## References

Ahnert F. 1967. The role of the equilibrium concept in the interpretation of landforms of fluvial erosion and deposition. In *L'evolution des versants*, Macar P (ed.). Liege, University of Liege: Liege; 23–41.

Ahnert F. 1987. Approaches to dynamic equilibrium in theoretical simulations of slope development. *Earth Surface Processes and landforms* **12**: 3–15.

Amundson R, Richter DD, Humphreys GS, Jobbagy EG, Gaillardet J. 2007. Coupling between biota and earth materials in the Critical Zone. *Elements* **3**: 327–332.

Anderson RS. 1994. Evolution of the Santa Cruz Mountains, California, through tectonic growth and geomorphic decay. *Journal of Geophysical Research – Solid Earth* **99**: 20161–20179.

Anderson RS. 2002. Modeling the tor-dotted crests, bedrock edges, and parabolic profiles of high alpine surfaces of the Wind River Range, Wyoming. *Geomorphology* **46**: 35–58.

Anderson SP, Dietrich WE. 2001. Chemical weathering and runoff chemistry in a steep headwater catchment. *Hydrological Processes* **15**: 1791–1815.

Anderson SP, Blum JD, Brantley SL, Chadwick O, Chorover J, Derry LA, Drever JI, Hering JG, Kirchner JW, Kump LR, Richter DD, White AF. 2004. Proposed initiative would study Earth's weathering engine. *EOS Transactions, American Geophysical Union* **85**: 265–269.

Anderson SP, von Blanckenburg F, White AF. 2007. Physical and chemical controls on the Critical Zone. *Elements* **3**: 315–319.

Balco G, Stone JO, Lifton NA, Dunai TJ. 2008. A complete and easily accessible means of calculating surface exposure ages or erosion rates from $^{10}$Be and $^{26}$Al measurements. *Quaternary Geochronology* **3**: 174.

Bierman P, Steig EJ. 1996. Estimating rates of denudation using cosmogenic isotope abundances in sediment. *Earth Surface Processes and Landforms* **21**: 125–139.

Bierman PR. 1994. Using in situ produced cosmogenic isotopes to estimate rates of landscape evolution; a review from the geomorphic perspective. *Journal of Geophysical Research, B, Solid Earth and Planets* **99**: 13885–13896.

Bierman PR. 2004. Rock to sediment – slope to sea with Be-10 – rates of landscape change. *Annual Review of Earth and Planetary Sciences* **32**: 215–255.

Bierman PR, Caffee M. 2002. Cosmogenic exposure and erosion history of Australian bedrock landforms. *Geological Society of America Bulletin* **114**: 787–803.

Brantley SL, Goldhaber MB, Ragnarsdottir KV. 2007. Crossing disciplines and scales to understand the Critical Zone. *Elements* **3**: 307–314.

Brown ET, Stallard RF, Larsen MC, Raisbeck GM, Yiou F. 1995. Denudation rates determined from the accumulation of in situ-produced $^{10}$Be in the Luquillo Experimental Forest, Puerto Rico. *Earth and Planetary Science Letters* **129**: 193–202.

Burkins DL, Blum JD, Brown K, Reynolds RC, Erel Y. 1999. Chemistry and mineralogy of a granitic, glacial soil chronosequence, Sierra Nevada Mountains, California. *Chemical Geology* **162**: 1–14.

Carson MA, Kirkby MJ. 1972. *Hillslope Form and Process*. Cambridge University Press: New York; 475 pp.

Child D, Elliott G, Mifsud C, Smith AM, Fink D. 2000. Sample processing for earth science studies at ANTARES. *Nuclear Instruments and Methods in Physics Research B* **172**: 856–860.

Cockburn HAP, Summerfield MA. 2004. Geomorphological applications of cosmogenic isotope analysis. *Progress in Physical Geography* **28**: 1–42.

Cox NJ. 1980. On the relationship between bedrock lowering and regolith thickness. *Earth Surface Processes and Landforms* **5**: 271–274.

Cull R, Hancock G, Johnston A, Martin P, Martin R, Murray AS, Pfitzner J, Warner RF, Wasson RJ. 1992. Past, present and future sedimentation on the Magela Plain and its catchment. In *Modern Sedimentation and Late Quaternary Evolution of the Magela Plain*, Wasson RJ (ed.), Supervising Scientist for the Alligator Rivers Region Research Report 6. AGPS: Canberra; 226–268.

Culling WEH. 1960. Analytical theory of erosion. *The Journal of Geology* **68**: 336–344.

Culling WEH. 1965. Theory of erosion on soil-covered slopes. *The Journal of Geology* **73**: 230–254.

Dietrich WE, Reiss R, Hsu M-L, Montgomery DR. 1995. A process-based model for colluvial soil depth and shallow landsliding using digital elevation data. *Hydrological Processes* **9**: 383–400.

Dietrich WE, Bellugi D, Heimsath AM, Roering JJ, Sklar L, Stock JD. 2003. Geomorphic transport laws for predicting landscape form and dynamics. In *Prediction in Geomorphology*, Wilcock P, Iverson R (eds), Volume Geophysical Monograph 135. American Geophysical Union: Washington, DC; 103–132.

Dietrich WE, Perron JT. 2006. The search for a topographic signature of life. *Nature* **439**: 411–418.

Erskine WD, Saynor MJ. 2000. *Assessment of the Off-site Geomorphic Impacts of Uranium Mining on Magela Creek, Northern Territory, Australia*, Supervising Scientist Report 156. Supervising Scientist: Darwin.

Fink D, Smith A. 2007. An inter-comparison of $^{10}$Be and $^{26}$Al AMS reference standards and the $^{10}$Be half-life. *Nuclear Instruments and Methods* **B259**: 600–609.

Gabet EJ, Reichman OJ, Seabloom EW. 2003. The effects of bioturbation on soil processes and sediment transport. *Annual Review of Earth and Planetary Sciences* **31**: 249–273.

Gilbert GK. 1877. *Report on the Geology of the Henry Mountains (Utah)*. United States Geological Survey: Washington, DC.

Gosse JC, Phillips FM. 2001. Terrestrial in situ cosmogenic nuclides: theory and application. *Quaternary Science Reviews* **20**: 1475–1560.

Granger DE, Kirchner JW, Finkel R. 1996. Spatially averaged long-term erosion rates measured from in situ-produced cosmogenic nuclides in alluvial sediment. *Journal of Geology* **104**: 249–257.

Hancock GR, Willgoose GR, Evans KG, Moliere DR, Saynor MJ. 2000. Medium term erosion simulation of an abandoned mine site using the SIBERIA landscape evolution model. *Australian Journal of Soil Research* **38**: 249–263.

Hancock GR, Loch RJ, Willgoose GR. 2003. The design of post-mining landscapes using geomorphic principles. *Earth Surface Processes and Landforms* **28**: 1097–1110.

Hancock GR, Evans KG. 2006. Gully position, characteristics and geomorphic thresholds in an undisturbed catchment in northern Australia. *Hydrological Processes* **20**: 2935–2951.

Hancock GR, Loughran RJ, Evans KG, Balog RM. 2008a. Estimation of soil erosion using field and modelling approaches in an undisturbed arnhem land catchment, Northern Territory, Australia. *Geographical Research* **46**: 333–349.

Hancock GR, Lowry JBC, Moliere DR, Evans KG. 2008b. An evaluation of an enhanced soil erosion and landscape evolution model: a case study assessment of the former Nabarlek uranium mine, Northern Territory, Australia. *Earth Surface Processes and Landforms* **33**: 2045–2063.

Hancock GR, Lowry JBC, Coulthard TJ, Evans KG, Moliere DR. in press. A catchment scale evaluation of the SIBERIA and CAESAR landscape evolution models. *Earth Surface Processes and Landforms*.

Heimsath AM, Dietrich WE, Nishiizumi K, Finkel RC. 1997. The soil production function and landscape equilibrium. *Nature* **388**: 358–361.

Heimsath AM, Dietrich WE, Nishiizumi K, Finkel RC. 1999. Cosmogenic nuclides, topography, and the spatial variation of soil depth. *Geomorphology* **27**: 151–172.

Heimsath AM, Chappell J, Dietrich WE, Nishiizumi K, Finkel RC. 2000. Soil production on a retreating escarpment in southeastern Australia. *Geology* **28**: 787–790.

Heimsath AM, Chappell J, Dietrich WE, Nishiizumi K, Finkel RC. 2001a. Late Quaternary erosion in southeastern Australia: a field example using cosmogenic nuclides. *Quaternary International* **83–85**: 169–185.

Heimsath AM, Dietrich WE, Nishiizumi K, Finkel RC. 2001b. Stochastic processes of soil production and transport: erosion rates, topographic variation, and cosmogenic nuclides in the Oregon Coast Range. *Earth Surface Processes and Landforms* **26**: 531–552.

Heimsath AM, Furbish DJ, Dietrich WE. 2005. The illusion of diffusion: field evidence for depth-dependent sediment transport. *Geology* **33**: 949–952.

Heimsath AM, Chappell J, Finkel RC, Fifield LK, Alimanovic A. 2006. Escarpment erosion and landscape evolution in southeastern Australia. *Geological Society of America Special Paper, Penrose Conference Series* **398**: 173–190.

Humphreys GS, Wilkinson MT. 2007. The soil production function: a brief history and its rediscovery. *Geoderma* **139**: 73–78.

Kaste JM, Heimsath AM, Bostick BC. 2007. Short-term soil mixing quantified with fallout radionuclides. *Geology* **35**: 243–246.

Lal D. 1988. In situ-produced cosmogenic isotopes in terrestrial rocks. Annual Review of Earth and Planetary Sciences **16**: 355–388.

Lal D. 1991. Cosmic ray labeling of erosion surfaces: in situ nuclide production rates and erosion models. *Earth and Planetary Science Letters* **104**: 424–439.

Lal D, Peters B. 1967. Cosmic ray produced radioactivity on the earth. *Encyclopedia of Physics* **XLVI**(2): 551–612.

Lal D, Arnold JR. 1985. Tracing quartz through the environment. Proceedings of the Indian Academy of Sciences (Earth Planetary Sciences) **94**: 1–5.

Matmon A, Shaked Y, Porat N, Enzel Y, Finkel R, Lifton N, Boaretto E, Agnon A. 2005. Landscape development in an hyperarid sandstone environment along the margins of the Dead Sea fault: implications from dated rock falls. *Earth & Planetary Science Letters* **240**: 803–817.

Minasny B, McBratney AB. 2001. A rudimentary mechanistic model for soil formation and landscape development II. A two-dimensional model incoporating chemical weathering. *Geoderma* **103**: 161–179.

Montgomery DR. 2007. Soil erosion and agricultural sustainability. *Proceedings of the National Academy of Sciences of the United States of America* **104**: 13268–13272.

Mudd SM, Furbish DJ. 2006. Using chemical tracers in hillslope soils to estimate the importance of chemical denudation under conditions of downslope sediment transport. *Journal of Geophysical Research – Earth Surface* **111**: F02021. DOI. 10.1029/2005JF000343

Nishiizumi K, Kohl CP, Klein J, Middleton R, Winterer EL, Lal D, Arnold JR. 1986. *In-situ 10 Be and 26 Al in Granitic Rocks with Glacially Polished Surfaces*, AGU 1986 fall meeting and ASLO winter meeting, volume 67, no. 44. Eos, Transactions, American Geophysical Union: San Francisco, CA; 1248.

Nishiizumi K, Kohl CP, Arnold JR, Klein J, Fink D, Middleton R. 1991. Cosmic ray produced $^{10}$Be and $^{26}$Al in Antarctic rocks; exposure and erosion history. *Earth and Planetary Science Letters* **104**: 440–454.

Nishiizumi K, Kohl CP, Arnold JR, Dorn R, Klein J, Fink D, Middleton R, Lal D. 1993. Role of in situ cosmogenic nuclides $^{10}$Be and $^{26}$Al in the study of diverse geomorphic processes. *Earth Surface Processes and Landforms* **18**: 407–425.

Nishiizumi K. *et al.* 2007. Absolute calibration of Be-10 AMS standards. *Nuclear Instruments & Methods in Physics Research Section B – Beam Interactions with Materials and Atoms* **258**: 403–413.

Riley SJ, Williams DK. 1991. Thresholds of gullying, Arnhem Land, Northern Territory. *Malaysian Journal of Tropical Agriculture* **22**: 133–143.

Saynor MJ, Erskine WD, Evans KG, Eliot I. 2004. Gully initiation and implications for management of scour holes in the vicinity of Jabiluka Mine, Northern Territory, Australia. *Geografiska Annaler Series A – Physical Geography* **86**: 191–203.

Saynor MJ, Staben G, Hancock G, Fox G, Calvert G, Smith B, Moliere DR, Evans KG. 2009. *Impact of Cyclone Monica on Catchments within the Alligator Rivers Region: Field Survey Data*, Internal Report 557, March, unpublished paper. Supervising Scientist: Darwin.

Small EE, Anderson RS, Hancock GS. 1999. Estimates of the rate of regolith production using $^{10}$Be and $^{26}$Al from an alpine hillslope. *Geomorphology* **27**: 131–150.

Staben G, Evans KG. 2008. Estimates of tree caopy loss as a result of Cyclone Monica, in the Magela Creek catchment nothern Australia. *Austral Ecology* **33**: 562–569.

Stone JO. 2000. Air pressure and cosmogenic isotope production. Journal of Geophysical Research **105**: 23753–23759.

Story R, Galloway RW, McAlpine JR, Aldrick JM, Williams MAJ. 1976. *Lands of the Alligator Rivers area, Northern Territory*, Land Research Series No. 38. CSIRO: Campbell.

Townsend SA, Douglas DD. 2000. The effect of three fire regimes on stream water quality, water yield and export coefficients in a tropical savanna (northern Australia). *Journal of Hydrology* **229**: 118–137.

Tucker GE, Slingerland R. 1997. Drainage basin responses to climate change. *Water Resources Research* **33**: 2031–2047.

van der Beek P, Braun J. 1999. Controls on post-mid-Cretaceous landscape evolution in the southeastern highlands of Australia: insights from numerical surface process models. *Journal of Geophysical Research* **104**: 4945–4966.

Wells T, Willgoose GR, Hancock GR. 2008. Modeling weathering pathways and processes of the fragmentation of salt weathered quartz-chlorite schist. *Journal of Geophysical Research – Earth Surface* **113**: F01014. DOI. 10.1029/2006JF000714

White AF, Blum AE, Schulz MS, Bullen TD, Harden JW, Peterson ML. 1996. Chemical weathering rates of a soil chronosequence on granitic alluvium. 1. Quantification of mineralogical and surface area changes and calculation of primary silicate reaction rates. *Geochimica et Cosmochimica Acta* **60**: 2533–2550.

White AF, Brantley SL. 2003. The effect of time on the weathering of silicate minerals: why do weathering rates differ in the laboratory and field? *Chemical Geology* **202**: 479–506.

Wilkinson MT, Humphreys GS. 2005. Exploring pedogenesis via nuclide-based soil production rates and OSL-based bioturbation rates. *Australian Journal of Soil Research* **43**: 767–779.

Wilkinson MT, Chappell J, Humphreys GS, Fifield K, Smith B, Hesse P. 2005. Soil production in heath and forest, Blue Mountains, Australia: influence of lithology and palaeoclimate. *Earth Surface Processes and Landforms* **30**: 923–934 (note: erratum correcting calculation errors and replotting data **30**: 1683–1685).

Yoo K, Amundson R, Heimsath AM, Dietrich WE, Brimhall GH. 2007. Integration of geochemical mass balance with sediment transport to calculate rates of soil chemical weathering and transport on hillslopes. *Journal of Geophysical Research – Earth Surface* **112**: F02013. DOI. 10.1029/2005JF000402